ISSN 0915-633X

9. 12. 9

9007

NATIONAL INSTITUTE FOR FUSION SCIENCE

The First Preliminary Experiments on an 84 GHz Gyrotron with a Single-Stage Depressed Collector

T. Shimozuma, M. Sato, Y. Takita, S. Ito, S. Kubo,
H. Idei, K. Ohkubo, T. Watari, T.S. Chu, K. Felch,
P. Cahalan and C.M. Loring, Jr

(Received - Oct. 3, 1997)

NIFS-513 Oct. 1997

RESEARCH REPORT
NIFS Series

NAGOYA, JAPAN

The First Preliminary Experiments on an 84GHz Gyrotron with a Single-Stage Depressed Collector

T. Shimozuma, M. Sato, Y. Takita, S. Ito, S. Kubo, H. Idei, K. Ohkubo, T. Watari, T. S. Chu[1], K. Felch[1], P. Cahalan[1] and C. M. Loring, Jr[1]

National Institute for Fusion Science
322-6, Oroshi-cho, Toki-shi, Gifu, 509-52, Japan
1) Communications & Power Industries, Inc.,
811 Hansen Way, Palo Alto, CA 94303 U.S.A.

Abstract

We fabricated and tested an 84GHz gyrotron with a single-stage depressed collector. The gyrotron has a high-voltage insulating section made of a low loss silicon nitride composite. In this preliminary experiment in the depressed collector configuration, we obtained 591kW, 41% operation with a depression voltage of 22.5kV. Access to the higher efficiency region was inhibited by an increase in anode current .

Keywords: electron cyclotron heating, gyrotron, depressed collector, electron beam

Introduction

High power, long pulse gyrotrons have succeeded in stable operation with a single-stage depressed collector[1,2]. The energy recovery of the spent electron beam by the depressed collector leads not only to an improvement in total output efficiency, but a reduction of the power loading and X-ray generation at the collector. When considering of pure CW high power gyrotrons, these merits are very attractive.

We have been developing an 84GHz CW gyrotron in collaboration with CPI for use as the power source in the ECRH system on LHD (Large Helical Device). Based on the previous success of the 84GHz CW gyrotron[3], we newly fabricated a gyrotron which has the same RF circuits, electron gun, and mode converter, but equipped with a depressed collector and larger Vacion pumps.

In this report, we describe the first experimental results of the 84GHz gyrotron in the depressed collector configuration.

84GHz gyrotron with a single-stage depressed collector

The 84GHz gyrotron has the same RF circuits, electron gun, built-in mode converter, and output window as the gyrotron which achieved 500kW-2sec., 400kW-10.5sec., 200kW-30sec., and 100kW CW operation. The oscillation mode in the cavity is $TE_{15,3}$, and the built-in mode converter system consists of a modified Vlasov launcher with visor and beam shaping mirrors. The output window is a sapphire double- disk window cooled by FC-75. A photograph of the gyrotron is shown in Fig. 1.

This gyrotron has been improved for high power CW operation: almost all parts of the body and collector sections are water-cooled, and two large 75 liter/second Vacion pumps improve the evacuating speed in

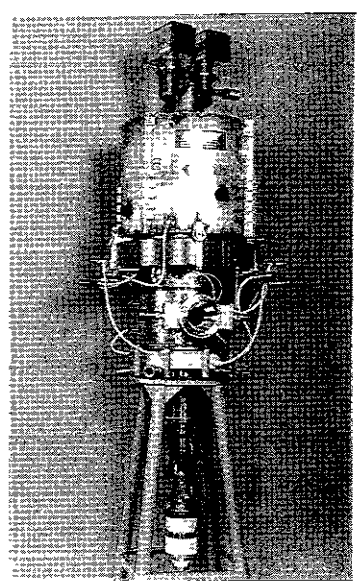

Figure 1 84GHz gyrotron with a depressed collector

the tube. The most remarkable difference is the addition of a high voltage insulating section between the body and the collector to be able to apply the retarding potential for the energy recovery of spent electrons.

The insulating section is made of a silicon nitride composite which has a low loss-tangent in the millimeter wave range[4]. Heat generation in this material can be reduced to less than one-third, compared with the usual alumina material. During CW operation, RF leakage from the insulating section is significant even though it is only a few percent of the output power. So the insulating section includes a cooling jacket which will allow lossy oil flow to cool the ceramic and absorb leaking RF.

Preliminary depressed collector experiments

Preliminary experiments were performed at the test set at CPI. During the first stage of gyrotron aging (normal operation without the retarding potential) the gyrotron achieved a maximum output power of 639kW and efficiency of 32% at beam voltage of 80kV and beam current of 25A for short pulses. During the normal operation, the insulating section was cooled by pure water so that power from RF leakage could be measured calorimetrically. It was about 0.7-1% of the total output power.

Since the gyrotron test set at CPI is not designed for depressed collector operation, a portable tetrode system was connected between the collector and grounded body to provide the depressed collector potential[5]. The test circuit is illustrated in Fig. 2. By adjusting the screen grid voltage of the tetrode, we were able to set the collector potential relative to the grounded gyrotron body. This system was only capable of operating at 0.5ms pulsewidth.

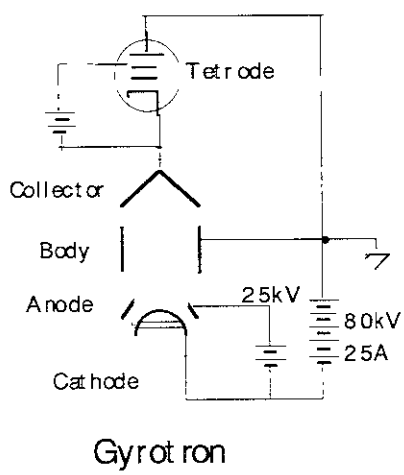

Figure 2 Circuit for depressed collector experiments

Figure 3 shows the dependence of the total and output oscillation efficiency on the depression voltage for several beam current operations. The total efficiency means the output efficiency included

an improvement by the depressed collector. On the other hand, the output efficiency corresponds to the one without the consideration of the depressed collector. At each point, the main accelerating voltage (potential difference between cathode and body) was set at 80kV, and the magnetic field and the anode voltage were optimized. For all beam current values, efficiency gradually increased as depression voltage was increased, until anode current was observed. Increasing the depression voltage beyond this point resulted in a drop in efficiency. Increased efficiency was due to energy recovery; the output efficiency actually remained constant or decreased slightly as voltage depression was increased. The highest efficiency achieved was 41.5% at 25kV of depression and 20A of beam current. At this point, output power was 475kW.

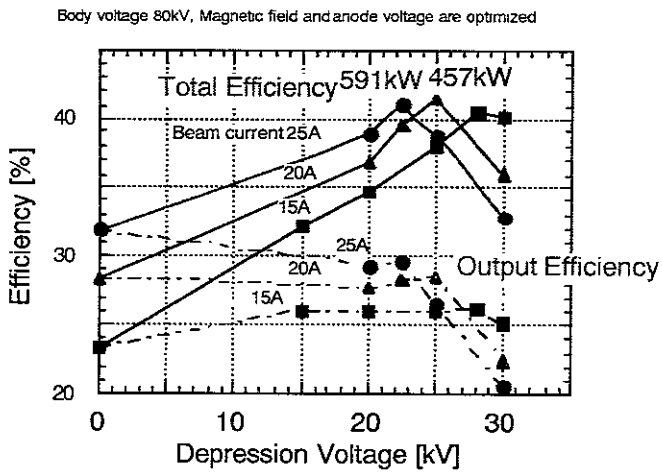

Figure 3 Total output efficiency is plotted as a function of depression voltage for several beam currents

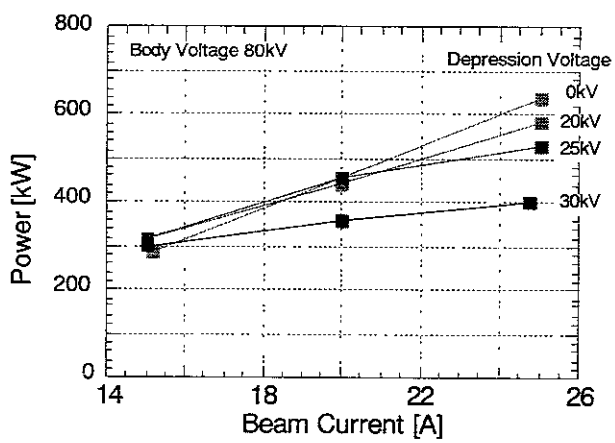

Figure 4 Dependence of output power on beam current for several depression voltages

Figure 4 shows the beam current dependence of the output power for several depression voltages. For zero depression voltage the output power increases with the beam current and reaches

640kW at 25A. For higher depression voltages, however, the increase of the output power is suppressed at high beam current. This tendency is more prominent for higher depression voltage.

Figure 5 shows the oscillation mode map for the beam current of 25A. Oscillation regions of the main mode ($TE_{15,3}$) are plotted for values of anode voltage and cavity coil current. In the figure each bounded area corresponds to the oscillation region with the application of the depression voltage indicated. The maximum output power values obtained for each depression voltage are also indicated in each region. This map illustrates the degradation of the oscillation efficiency at higher depression voltages. When the depression voltage increases, the anode voltage corresponding to the anode current onset decreases, and the region shrinks to the lower anode voltage and higher magnetic field side. As a result, the gyrotron could not be operated in the higher efficiency region.

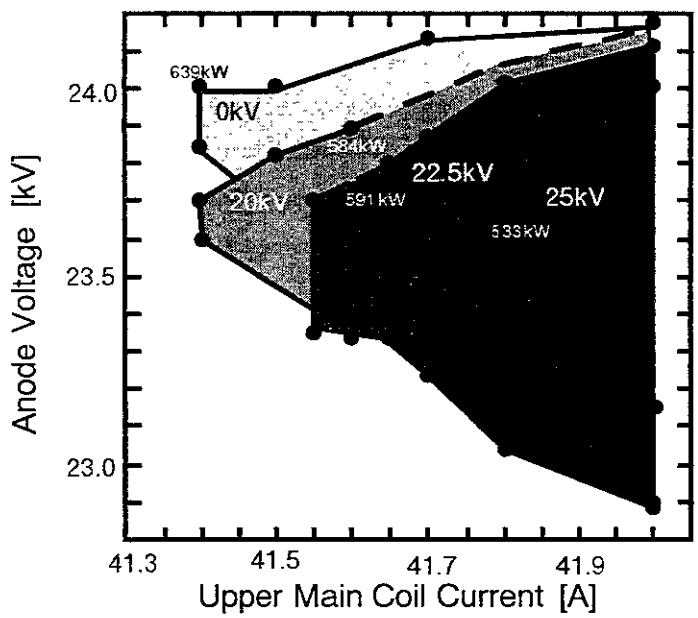

Figure 5 Oscillation mode map for depression voltage of 0, 20,22.5,25kV

This tube is now being aged at the NIFS test set to obtain several hundred kilowatts CW without depression. Long pulse testing in the depressed collector configuration will be conducted in near future.

Summary

We fabricated and made preliminary tests of an 84GHz gyrotron with a single-stage depressed collector. The gyrotron has a high-voltage insulating section made of a low loss silicon nitride composite. Leakage RF from the insulating section was measured to be 0.7-1% of the output power. In this preliminary experiment in the depressed collector configuration, we obtained 591kW, 41%

operation with a depression voltage of 22.5kV at a beam current of 25A, in contrast with 32% without retarding voltage. Access to the higher efficiency region was inhibited by the anode current increase.

References

[1] K. Sakamoto, M. Tsuneoka, A. Kasugai, T. Imai, T. Kariya, K. Hayashi, and Y. Mitsunaka, *"Major Improvement of Gyrotron Efficiency with Beam Energy Recovery"*, Phys. Rev. Lett., 73(1994)3532-3535.

[2] B. Piosczyk, C. T. Iatrou, G. Dammertz, and M. Thumm, *"Single-Stage Depressed Collectors for Gyrotron"*, IEEE Trans. on Plasma Science 24(1996)579-585.

[3] M. Sato, T. Shimozuma, Y. Takita, S. Kubo, H. Idei, K. Ohkubo, T. Kuroda, T. Watari, M. Loring, Jr, S. Chu, K. Felch and H. Huey, "Development *of a High Power, 84GHz CW Gyrotron",* Conference Digest of the 20th International Conference on Infrared and Millimeter Waves, Orlando, Florida, December 11-14, 1995 T4.3, pp195-196

[4] T. Shimozuma, M. Sato, Y. Takita, S. Kubo, H. Idei, K. Ohkubo, T. Watari, S. Morimoto and K. Tajima, *"Development of Elongated Vacuum Windows for High Power CW Millimeter Waves",* Conference Digest of the 20th International Conference on Infrared and Millimeter Waves, Orlando, Florida, December 11-14, 1995 T8.3, pp273-274.

[5] R. L. Ives, H. R. Jory, J. Neilson, M. Chodorow, J. Feinstein, A. D. LaRue, Z. Zitelli, and R. Martorana, *"Development and Test of a 500-kW, 8-GHz Gyrotron"*, IEEE Trans. on Electron Devices, 40(1993)1316-1321.

Recent Issues of NIFS Series

NIFS-466 H. Miura and S. Kida,
Identification of Tubular Vortices in Complex Flows; Dec. 1996

NIFS-467 Y. Takeiri, Y. Oka, M. Osakabe, K. Tsumori, O. Kaneko, T. Takanashi, E. Asano, T. Kawamoto, R. Akiyama and T. Kuroda,
Suppression of Accelerated Electrons in a High-current Large Negative Ion Source; Dec. 1996

NIFS-468 A. Sagara, Y. Hasegawa, K. Tsuzuki, N. Inoue, H. Suzuki, T. Morisaki, N. Noda, O. Motojima, S. Okamura, K. Matsuoka, R. Akiyama, K. Ida, H. Idei, K. Iwasaki, S. Kubo, T. Minami, S. Morita, K. Narihara, T. Ozaki, K. Sato, C. Takahashi, K. Tanaka, K. Toi and I. Yamada,
Real Time Boronization Experiments in CHS and Scaling for LHD; Dec. 1996

NIFS-469 V.L. Vdovin, T.Watari and A. Fukuyama,
3D Maxwell-Vlasov Boundary Value Problem Solution in Stellarator Geometry in Ion Cyclotron Frequency Range (final report); Dec. 1996

NIFS-470 N. Nakajima, M. Yokoyama, M. Okamoto and J. Nührenberg,
Optimization of M=2 Stellarator; Dec. 1996

NIFS-471 A. Fujisawa, H. Iguchi, S. Lee and Y. Hamada,
Effects of Horizontal Injection Angle Displacements on Energy Measurements with Parallel Plate Energy Analyzer; Dec. 1996

NIFS-472 R. Kanno, N. Nakajima, H. Sugama, M. Okamoto and Y. Ogawa,
Effects of Finite-β and Radial Electric Fields on Neoclassical Transport in the Large Helical Device; Jan. 1997

NIFS-473 S. Murakami, N. Nakajima, U. Gasparino and M. Okamoto,
Simulation Study of Radial Electric Field in CHS and LHD; Jan. 1997

NIFS-474 K. Ohkubo, S. Kubo, H. Idei, M. Sato, T. Shimozuma and Y. Takita,
Coupling of Tilting Gaussian Beam with Hybrid Mode in the Corrugated Waveguide; Jan. 1997

NIFS-475 A. Fujisawa, H. Iguchi, S. Lee and Y. Hamada,
Consideration of Fluctuation in Secondary Beam Intensity of Heavy Ion Beam Prove Measurements; Jan. 1997

NIFS-476 Y. Takeiri, M. Osakabe, Y. Oka, K. Tsumori, O. Kaneko, T. Takanashi, E. Asano, T. Kawamoto, R. Akiyama and T. Kuroda,
Long-pulse Operation of a Cesium-Seeded High-Current Large Negative Ion Source; Jan. 1997

NIFS-477 H. Kuramoto, K. Toi, N. Haraki, K. Sato, J. Xu, A. Ejiri, K. Narihara, T. Seki, S. Ohdachi,

K. Adati, R. Akiyama, Y. Hamada, S. Hirokura, K. Kawahata and M. Kojima,
Study of Toroidal Current Penetration during Current Ramp in JIPP T-IIU with Fast Response Zeeman Polarimeter; Jan., 1997

NIFS-478 H. Sugama and W. Horton,
Neoclassical Electron and Ion Transport in Toroidally Rotating Plasmas; Jan. 1997

NIFS-479 V.L. Vdovin and I.V. Kamenskij,
3D Electromagnetic Theory of ICRF Multi Port Multi Loop Antenna; Jan. 1997

NIFS-480 W.X. Wang, M. Okamoto, N. Nakajima, S Murakami and N. Ohyabu,
Cooling Effect of Secondary Electrons in the High Temperature Divertor Operation; Feb. 1997

NIFS-481 K. Itoh, S.-I. Itoh, H. Soltwisch and H.R. Koslowski,
Generation of Toroidal Current Sheet at Sawtooth Crash; Feb. 1997

NIFS-482 K. Ichiguchi,
Collisionality Dependence of Mercier Stability in LHD Equilibria with Bootstrap Currents; Feb. 1997

NIFS-483 S. Fujiwara and T. Sato,
Molecular Dynamics Simulations of Structural Formation of a Single Polymer Chain: Bond-orientational Order and Conformational Defects; Feb. 1997

NIFS-484 T. Ohkawa,
Reduction of Turbulence by Sheared Toroidal Flow on a Flux Surface; Feb. 1997

NIFS-485 K. Narihara, K. Toi, Y. Hamada, K. Yamauchi, K. Adachi, I. Yamada, K. N. Sato, K. Kawahata, A. Nishizawa, S. Ohdachi, K. Sato, T. Seki, T. Watari, J. Xu, A. Ejiri, S. Hirokura, K. Ida, Y. Kawasumi, M. Kojima, H. Sakakita, T. Ido, K. Kitachi. J. Koog and H. Kuramoto,
Observation of Dusts by Laser Scattering Method in theJIPPT-IIU Tokamak Mar. 1997

NIFS-486 S. Bazdenkov, T. Sato and The Complexity Simulation Group,
Topological Transformations in Isolated Straight Magnetic Flux Tube; Mar. 1997

NIFS-487 M. Okamoto,
Configuration Studies of LHD Plasmas; Mar. 1997

NIFS-488 A. Fujisawa, H. Iguchi, H. Sanuki, K. Itoh, S. Lee, Y. Hamada, S. Kubo, H. Idei, R. Akiyama, K. Tanaka, T. Minami, K. Ida, S. Nishimura, S. Morita, M. Kojima, S. Hidekuma, S.-I. Itoh, C. Takahashi, N. Inoue, H. Suzuki, S. Okamura and K. Matsuoka,
Dynamic Behavior of Potential in the Plasma Core of the CHS

Heliotron/Torsatron; Apr. 1997

NIFS-489 T. Ohkawa,
Pfirsch - Schlüter Diffusion with Anisotropic and Nonuniform Superthermal Ion Pressure; Apr. 1997

NIFS-490 S. Ishiguro and The Complexity Simulation Group,
Formation of Wave-front Pattern Accompanied by Current-driven Electrostatic Ion-cyclotron Instabilities; Apr. 1997

NIFS-491 A. Ejiri, K. Shinohara and K. Kawahata,
An Algorithm to Remove Fringe Jumps and its Application to Microwave Reflectometry; Apr. 1997

NIFS-492 K. Ichiguchi, N. Nakajima, M. Okamoto,
Bootstrap Current in the Large Helical Device with Unbalanced Helical Coil Currents; Apr. 1997

NIFS-493 S. Ishiguro, T. Sato, H. Takamaru and The Complexity Simulation Group,
V-shaped dc Potential Structure Caused by Current-driven Electrostatic Ion-cyclotron Instability; May 1997

NIFS-494 K. Nishimura, R. Horiuchi, T. Sato,
Tilt Stabilization by Energetic Ions Crossing Magnetic Separatrix in Field-Reversed Configuration; June 1997

NIFS-495 T. -H. Watanabe and T. Sato,
Magnetohydrodynamic Approach to the Feedback Instability; July 1997

NIFS-496 K. Itoh, T. Ohkawa, S. -I.Itoh, M. Yagi and A. Fukuyama
Suppression of Plasma Turbulence by Asymmetric Superthermal Ions; July 1997

NIFS-497 T. Takahashi, Y. Tomita, H. Momota and Nikita V. Shabrov,
Collisionless Pitch Angle Scattering of Plasma Ions at the Edge Region of an FRC; July 1997

NIFS-498 M. Tanaka, A.Yu Grosberg. V.S. Pande and T. Tanaka,
Molecular Dynamics and Structure Organization in Strongly-Coupled Chain of Charged Particles; July 1997

NIFS-499 S. Goto and S. Kida,
Direct-interaction Approximation and Reynolds-number Reversed Expansion for a Dynamical System; July 1997

NIFS-500 K. Tsuzuki, N. Inoue, A. Sagara, N. Noda, O. Motojima, T. Mochizuki, T. Hino and T. Yamashina,
Dynamic Behavior of Hydrogen Atoms with a Boronized Wall; July 1997

NIFS-501 I. Viniar and S. Sudo,
Multibarrel Repetitive Injector with a Porous Pellet Formation Unit; July 1997

NIFS-502 V. Vdovin, T. Watari and A. Fukuyama,
An Option of ICRF Ion Heating Scenario in Large Helical Device; July 1997

NIFS-503 E. Segre and S. Kida,
Late States of Incompressible 2D Decaying Vorticity Fields; Aug. 1997

NIFS-504 S. Fujiwara and T. Sato,
Molecular Dynamics Simulation of Structural Formation of Short Polymer Chains; Aug. 1997

NIFS-505 S. Bazdenkov and T. Sato
Low-Dimensional Model of Resistive Interchange Convection in Magnetized Plasmas; Sep. 1997

NIFS-506 H. Kitauchi and S. Kida,
Intensification of Magnetic Field by Concentrate-and-Stretch of Magnetic Flux Lines; Sep. 1997

NIFS-507 R.L. Dewar,
Reduced form of MHD Lagrangian for Ballooning Modes; Sep. 1997

NIFS-508 Y.-N. Nejoh,
Dynamics of the Dust Charging on Electrostatic Waves in a Dusty Plasma with Trapped Electrons; Sep.1997

NIFS-509 E. Matsunaga, T.Yabe and M. Tajima,
Baroclinic Vortex Generation by a Comet Shoemaker-Levy 9 Impact; Sep. 1997

NIFS-510 C.C. Hegna and N. Nakajima,
On the Stability of Mercier and Ballooning Modes in Stellarator Configurations; Oct. 1997

NIFS-511 K. Orito and T. Hatori,
Rotation and Oscillation of Nonlinear Dipole Vortex in the Drift-Unstable Plasma; Oct. 1997

NIFS-512 J. Uramoto,
Clear Detection of Negative Pionlike Particles from H_2 Gas Discharge in Magnetic Field; Oct. 1997

NIFS-513 T. Shimozuma, M. Sato, Y. Takita, S. Ito, S. Kubo, H. Idei, K. Ohkubo, T. Watari, T.S. Chu, K. Felch, P. Cahalan and C.M. Loring, Jr,
The First Preliminary Experiments on an 84 GHz Gyrotron with a Single-Stage Depressed Collector; Oct. 1997